Reverse time migration with causal imaging condition using an improved method to calculate the analytical wavefield

Daniel Revelo *, CPGG/UFBA,   Reynam C. Pestana, CPGG/UFBA

Abstract

In this work the analytical wavefield is computed by just solving the wave equation once, differently of conventional methods that need to solve the wave equation twice: once for the source and another for the Hilbert transformed source. Our proposed method can improve the computation of wavefield separation and can bring the causal imaging condition into practice. For time extrapolation, we are using the rapid expansion method to compute the wavefield and its first order time derivative and then compute the analytical wavefield. This method is unconditionally stable and free of numerical noise. By computing the analytical wavefield, we can, therefore, separate the wavefield into down- and up-going components for each time step in an explicit way. For RTM applications, we can now employ the causal imaging condition and through a synthetic example, we could demonstrate the effectiveness of this new imaging condition without applying a Laplacian filter. The RTM result shows that it can successfully remove the low-frequency noise which is common in the typical cross-correlation imaging condition.

Introduction

In the traditional reverse time migration (RTM), the source and receive wavefields are forward and backward propagated and respectively correlated along the time axis at zero lag. The resulting image obtained by applying the conventional cross-correlation between source and receiver wavefields is always contaminated by low spatial-low-frequency artifacts due to the presence of sharp wave-speed contrasts in the velocity model. In recent years, more attention has been given to improve the imaging condition and reduce the low frequency noise. Different techniques have been proposed in the literature (Baysal et al., 1984; Yoon and Marfurt, 2006; Fletcher et al., 2006; Guitton et al., 2007). A practical approach that is easy to apply is the Laplacian filter (Zhang and Sun, 2009), which shows good attenuation but it can damage the signal of interest (Guitton et al., 2007).

Another way to address this type of migration artefact is to modify the imaging condition. In this direction, Liu et al. (2011) proposed an imaging condition based on the decomposition of the wavefield into one-way components. The imaging condition introduced by Liu et al. (2011) only allows waves components that propagate in opposite directions to be correlated. Liu's method is an implicit separation which successfully removes many types of artifacts without a Laplacian filter.

To address the wavefield separation, we usually define the wave-propagation direction in the Fourier domain. In the frequency-wavenumber domain, the wave-propagation is defined by the sign of the frequency and the wavenumber (Hu and McMechan, 1987; Liu et al., 2011). If we use the conventional wavefield decomposition method in the time-domain RTM, we should store the wavefield and perform Fourier transform along the time axis. This process increase the input/output cost, because the time axis is the slowest dimension of the stored wavefield and Fourier transform operates most efficiently on data that are stored contiguously. But, if we can define a time-domain wavefield whose spectrum only contains a positive or negative frequency, we can define the wave-propagation direction using the sign of the spatial wavenumber and avoid the I/O cost. This signal is the analytical signal which is widely used in signal processing. The analytical signal is a complex signal whose real part is the signal itself and its complex part is the Hilbert transform of the real part. For RTM, we extend the analytic signal concept and call it the analytical wavefield.

In a recent paper presented by Shen and Albertin (2015) the imaginary part of the analytical wavefield is obtained applying a temporal Hilbert transform to the source term of the wave-equation followed by conventional propagation. The pair of wavefield, the wavefield propagated with conventional source and the wavefield generated by its Hilbert transform, constitute the analytical wavefield. Because the analytical wavefield only contains positive frequencies, the down- and up-going wave components can then be conveniently obtained by applying 1D Fourier filters in depth. Shen and Albertin (2015) propose a causal imaging condition that correlates the down-going source component with the up-going receiver component for subsurface imaging. This method was tested and it successfully removed many types of salt-imaging artifacts presented in the images obtained from conventional cross-correlation imaging condition (Claerbout, 1971).

Revelo et al. (2016) applied the one-step extrapolation (OSE) method to compute the analytical wavefield. For reverse time migration (RTM) both source and receiver wavefields were extrapolated in time and the source and receiver wavefields were separated in their down- and up-going components for each time step in an explicit way based on Shen and Albertin (2015) method. The clear distintion between Revelo et al. (2016) method and the one proposed by Shen and Albertin (2015) is that Revelo et al. (2016) use a first order wave-equation solution injecting

an analytical source wavefield, while Shen and Albertin (2015) needs to solve the wave equation twice: once for the source and another for the Hilbert transform of the source. As with respect to the work of Liu et al. (2011), the major difference is that the method proposed by Shen and Albertin (2015) and also used by Revelo et al. (2016) can provide an explicit separation of the wavefield, while Liu's method uses an implicit separation.

In this paper, we are proposing to compute the analytical wavefield using the rapid expansion method (REM) (Pestana and Stoffa, 2010). The REM propagates waves free of numerical dispersion noise and it is able to extrapolate waves in time using a time step up to Nyquist's limit. With the REM we can also obtain the first order time derivative of the wavefield at the same time step and thus compute the Hilbert transform of the wavefield as proposed by Zhang and Zhang (2009). After that, we can separate the wavefields into its down- and up-going components. In our proposed method, the wave equation is only solved once, improving the computational efficiency of the wavefield separation procedure and therefore the application of the causal imaging condition for RTM.

Theory

The zero-lag cross-correlation between the extrapolated source (S) and receiver (R) wavefields is the imaging condition conventionally used in RTM. This imaging condition was proposed originally by Claerbout (1971) and is defined as follows:

$$I_{cc}(\mathbf{x}) = \int_0^T S(\mathbf{x},t)\, R(\mathbf{x},t)\, dt \qquad (1)$$

where $\mathbf{x} = (x,z)$, T is the total time the and I_{cc} is the cross-correlation image.

In order to avoid the low-frequency noise produced by the cross-correlation imaging condition, Revelo et al. (2016) used a causal imaging condition that correlates the down-going component of the source, S_d, with the up-going component of receiver wavefield, R_u, as proposed by Shen and Albertin (2015):

$$I_{causal}(\mathbf{x}) = \int_0^T S_d(\mathbf{x},t)\, R_u(\mathbf{x},t)\, dt \qquad (2)$$

This imaging condition correlates wavefields only in points in space that correspond to seismic reflectors, avoiding noise along wavepaths and artifacts which are typical from the conventional RTM.

To obtain the individual components involved in Eq. 2, we need to introduce an analytical wavefield. The complex (analytical) wavefield is defined as $\hat{P} = P(\mathbf{x},t) + iQ(\mathbf{x},t)$, where $Q(\mathbf{x},t) = H\{P(\mathbf{x},t)\}$ and $H\{\cdot\}$ is the Hilbert transform operator. For general media, this complex pressure wavefield $\hat{P}$ satisfy a first-order partial equation in time (Zhang and Zhang, 2009).

Following Zhang and Zhang (2009), the relation between Q and P can be expressed as

$$Q(\mathbf{x},t) = \frac{1}{L}\frac{\partial P(\mathbf{x},t)}{\partial t} \qquad (3)$$

where L is a pseudo-differential operator in the space domain, defined by $L = v(\mathbf{x})\sqrt{-\nabla^2}$ and ∇^2 is Laplacian

operator. Its symbolic representation is $L = v(\mathbf{x})\sqrt{k_x^2 + k_z^2}$ where k_x and k_z are the wave number components and $v(\mathbf{x})$ is the propagation velocity in the medium.

More recently, Revelo et al. (2016) used the one-step extrapolation (OSE) method to compute the analytical wavefield which takes as base the solution of a first order wave-equation injecting an analytical source wavefield. Another different procedure was also proposed by Shen and Albertin (2015) to compute the analytical wavefield, but in their case the wave equation has to be solved twice, once for the source and another for the Hilbert transformed source.

As cited by Shen and Albertin (2015) the Hilbert transformed H_t commutes with the wave-equation operator and we have that:

$$H_t\left(\frac{1}{v^2}\partial_t^2 - \nabla^2\right)P = \left(\frac{1}{v^2}\partial_t^2 - \nabla^2\right)H_t P = H_t f \qquad (4)$$

where v is the velocity and f is the source wavelet. Thus, we can get the imaginary part of the analytical wavefield by solving the wave-equation with its source term Hilbert transformed in forward time.

Here, we are proposing to compute the analytical wavefield solving the wave equation only once. For this, in order to solve the acoustic wave equation in time, we consider the rapid expansion method (REM) proposed by Pestana and Stoffa (2010), in which the wavefield is found through the propagation scheme

$$
\begin{aligned}
P(\mathbf{x},t+\Delta t) &= -P(\mathbf{x},t-\Delta t) \\
&+ 2\left[\sum_{k=0}^M c_{2k} J_{2k}(\Delta t R) Q_{2k}\left(\frac{iL}{R}\right)\right]P(\mathbf{x},t) \quad (5)
\end{aligned}
$$

where $-L^2 = v^2(\mathbf{x})\nabla^2$, $c_0 = 1$ and $c_k = 2$ if $k \neq 0$. The value J_{2k} represents the Bessel function of order $2k$, the Q_{2k} are modified Chebyshev polynomials and the term R is a scalar larger than the range of eigenvalues of $-L^2$. The REM provides a solution with very high degree of accuracy and can be reduced to various finite-difference time-derivative schemes.

Tessmer (2011) showed that with the help of Eq. 5 the time derivative of the pressure field can be obtained. Taking into account that the only time-dependent term in the expansion of the Eq. 5 is the Bessel function, we can obtain the first time derivative of the wavefield in the following form:

$$
\begin{aligned}
\dot{P}(\mathbf{x},t+\Delta t) &= \dot{P}(\mathbf{x},t-\Delta t) \qquad (6) \\
&+ 2\left[\sum_{k=0}^M c_{2k} R \frac{d}{d\tau} J_{2k}(\tau = \Delta t R) Q_{2k}\left(\frac{iL}{R}\right)\right]P(\mathbf{x},t)
\end{aligned}
$$

Using the REM solution, we can compute for each time-step the wavefield and its first order time derivative. Afterwards, using Eq. 3 we compute the Hilbert transform wavefield for both source and receivers and get the analytical wavefield for each step in time needed for the wavefield separation and application of the causal imaging condition.

Explicit wavefield separation for causal imaging condition

In the causal imaging condition the down-going component of source wavefield, S_d, and the up-going component of receiver wavefield, R_u, are correlated to obtain the resulting imaging using Eq. 2. To obtain individual wavefield components involved in Eq. 2, following Shen and Albertin (2015), we use a Fourier transform in depth of the analytical wavefield considering mono frequency components (Liu et al., 2011). The down-going component of source wavefield, S_d, in space and time becomes

$$S_d(x,z,t) = \frac{1}{2\pi}\Re \int_{-\infty}^{+\infty}\int_{-\infty}^{+\infty} \hat{S}(x,z',t)e^{ik_z(z-z')}\kappa(k_z)dz'dk_z, \quad (7)$$

where,

$$\kappa(k_z) = \begin{cases} 0 & \text{if } k_z \geq 0 \\ 1 & \text{if } k_z < 0 \end{cases} \quad (8)$$

and $\hat{S}$ is the source analytical wavefield.

The up-going receiver wavefield component in forward time, R_u, is obtained using the analytical receiver wavefield in Eq. 7 and replacing κ by $1 - \kappa$. Shen and Albertin (2015) solved the real and the imaginary part of the source analytical wavefield individually from the wave equation with its source term corresponding to the original source wavelet and its Hilbert transform in time, respectively.

In summary, in our implementation we are proposing to use the REM method to obtain the real part of the wavefield through Eq. 5. Inside the time step loop, the imaginary part of analytical wavefield is computed based on Eqs. 6 and 3. After that, we can separate the wavefields into down- and up-going components of source and receiver wavefields. Thus, avoiding to solve the wave equation twice what can improve the computational efficiency of the wavefield separation procedure and therefore the application of the causal imaging condition for RTM.

Numerical examples

We use a three-layer model to compare the conventional wavefield separation and the procedure proposed in this work. The 2D model consists of 256×256 grid nodes with $20\,\mathrm{m}$ grid spacing. The depth of the layers are 1.5, 2.5 and $3.5\,\mathrm{km}$ with velocities of 1500, 2500 and $3500\,\mathrm{m/s}$, respectively. To test the separation procedure, we injected a source wavelet with a $30\,\mathrm{Hz}$ cut-off frequency at the center of the model with a time sampling of $2\,\mathrm{ms}$. For comparison, we show on Figure 1 the real and the complex parts of the analytical wavefield (Figures 1a and 1c) and also the up-going (reflected waves - Figure 1e) and down-going components (transmitted waves - Figure 1g), which were obtained through the propagation of both the source and the Hilbert transformed source (two propagation). Ever using the method proposed, just a single propagation by REM, we can compute the real wavefield and its Hilbert transform by Eq. 3, resulting in the analytical wavefield. The real and complex parts of the analytical wavefield (Figures 1b and 1d) and the up- and down-going components, Figures 1f and 1h, respectively, are shown on the right part of the Figure 1. We notice that the images are similar in quality, proving that the results obtained for both procedures are equivalents. Moreover, with these

results we demonstrate that the analytical wavefield can be computed by solving the wave equation just for an injected source, as proposed.

(a) Real part.   (b) Real part.

(c) Complex part.   (d) Complex part.

(e) Up-going component.   (f) Up-going component.

(g) Down-going component.   (h) Down-going component.
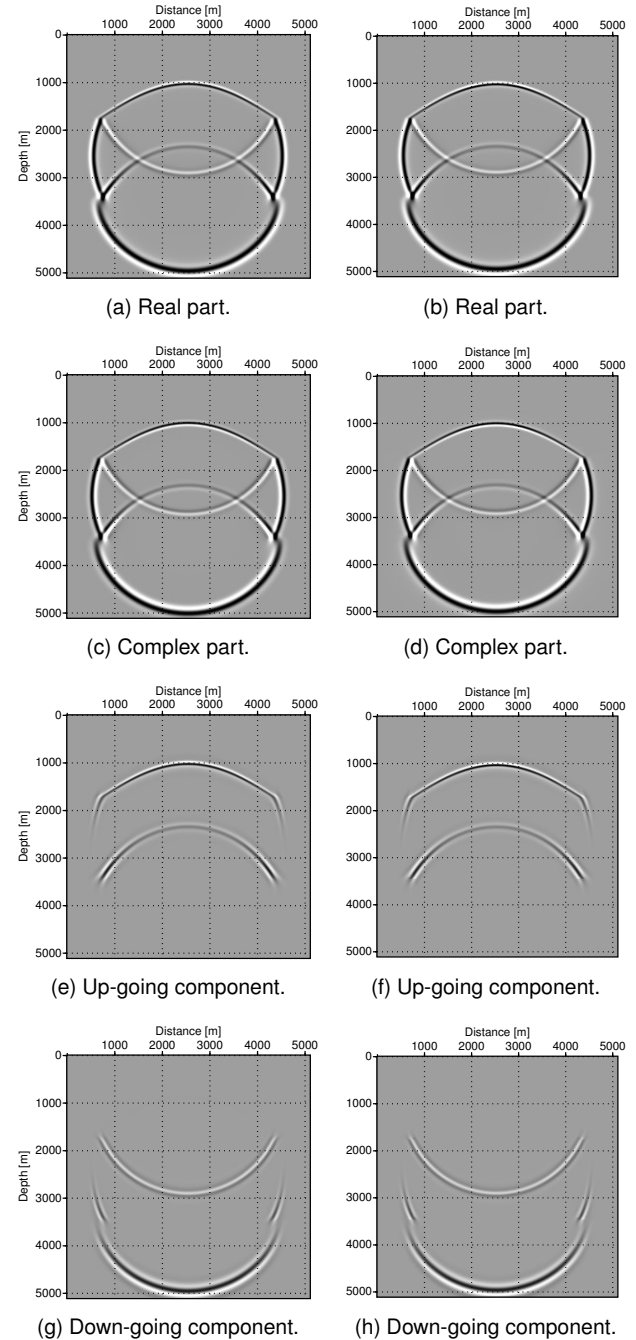
Figure 1: Snapshots for source wavefields at $t = 0.862\,\mathrm{s}$ for the real and complex parts and for the up- and down-going wavefields. Figures on the left were obtained using a source and the Hilbert transformed source - two propagations. Figures on the right were obtained using Eqs. 6 and 3 - by the REM using only a single propagation.

As a validation of the method developed in this work, we apply the RTM with the causal imaging condition for the dataset of the fault model shown in Figure 3(a). The fault model is characterized by several faults, as well as

a complicated base, with the presence of intrusions. The numerical discretization contains 600×230 samples, with spacing of $20\,\mathrm{m}$ in both directions. This is a high-quality dataset generated by REM modeling with shot spacing of $40\,\mathrm{m}$, receiver spacing of $20\,\mathrm{m}$, and $2560\,\mathrm{m}$ maximum offset. In the migration, the highest frequency was $50\,\mathrm{Hz}$ and the time step of $\Delta t = 4\,\mathrm{ms}$. Figure 3 shows the comparison of the migration results obtained by cross-correlation imaging condition, using the conventional way to compute the analytical wavefield and the method proposed in the present work. For such a dataset, the results show that our method can handle complex velocity fairly well and gives good delineation at the faults, specially at the main fault, as well as the domes and the horizontal plane at the bottom . Theses results confirm the successful application of RTM, using REM for forward and backward propagation, combined with the computation of the analytical wavefield which allow us to separate the wavefield for application of the causal imaging condition. Furthermore, showing the effectiveness of the implemented algorithm for removing noise, usually seen in a typical reverse-time migration imaging (Figure 3b).

The migrated time consumed by each method is presented in the Figure 2 for the fault model dataset. It is observed that the time consumed by the present method - single propagation - is less than the time consumed by the conventional method used in the calculation of the analytical wavefield. Therefore, the method we are proposing here can bring the causal imaging condition for RTM at lower computational cost and still providing similar results when compared to the conventional method.
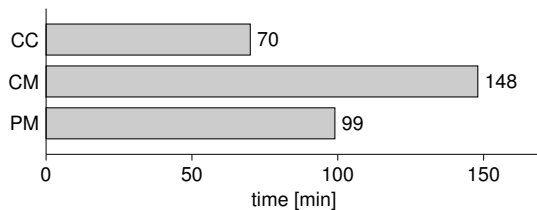
Figure 2: Total migration time. CC: conventional cross-correlation, CM: causal imaging condition and PM: causal imaging condition applying the proposed method.

Conclusions

We have shown a new procedure to compute the analytical wavefield based on the rapid expansion method in a stable way and free of dispersion noise. In our proposed method the source wavefield is extrapolated in time and for each time step we can compute the first order time derivative and then the Hilbert transform of the wavefield. From the results obtained for the complex fault model we have demonstrated that we can compute the analytical wavefield using just a single propagation at the same quality of the conventional procedure using two propagations. Moreover, using an algorithm to explicitly separate the wavefield into up- and down-going components, we can apply the causal imaging condition for RTM in a very low computation cost. Furthermore, we demonstrated using the fault model data set that the causal imaging condition can effectively remove the undesired low-frequency noise produced by the cross-correlation imaging condition.
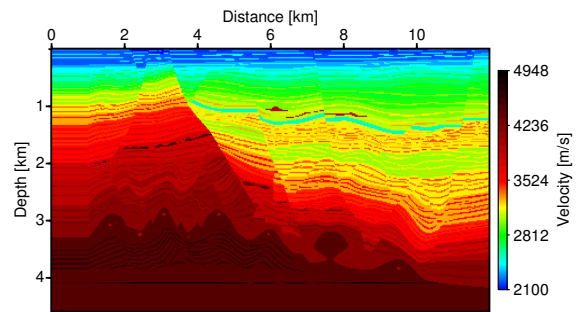
(a) Fault model.
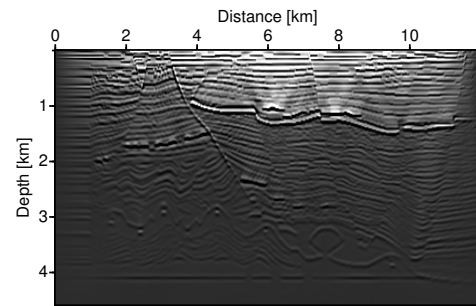
(b) Conventional imaging condition.
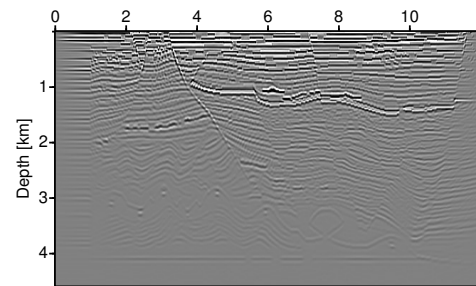
(c) Conventional imaging condition with Laplacian filter.
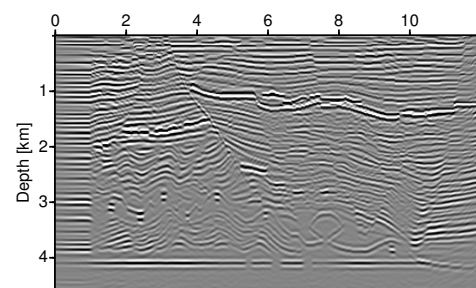
(d) Analytical wavefield by conventional procedure.
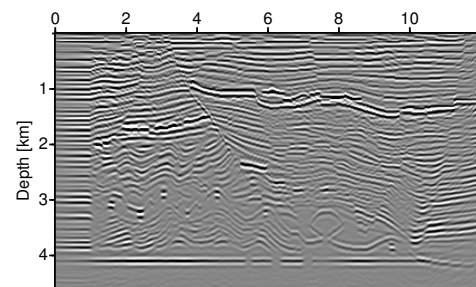
(e) With the proposed method.

Figure 3: Reverse time migration results using the REM. (b) and (c) are images obtained by applying the conventional cross-correlation imaging condition and (d) and (e) by the causal imaging condition.

Acknowledgements

References

Baysal, E., D. D. Kosloff, and J. W. C. Sherwood, 1984, A two-way nonreflecting wave equation: Geophysics, **49**, 132–141.

Claerbout, J., 1971, Toward a unified theory of reflector mapping: Geophysics, **36**, 467481.

Fletcher, R., P. Fowler, P. Kitchenside, and U. Albertin, 2006, Suppressing unwanted internal reflections in prestack reverse-time migration: Geophysics, **71**, E79–E82.

Guitton, A., B. Kaelin, and B. Biondi, 2007, Least-squares attenuation of reverse-time migration artifacts: Geophysics, **72**, S19–S23.

Hu, L. and G. A. McMechan, 1987, Wave-field transformations of vertical seismic profiles: Geophysics, **52**, 307–321.

Liu, F., G. Zhang, S. Morton, and J. Leveille, 2011, An effective imaging condition for reverse-time migration using wavefield decomposition: Geophysics, **76**, S29–S39.

Pestana, R. and P. Stoffa, 2010, Time evolution of the wave equation using rapid expansion method: Geophysics, **75**, T121–T131.

Revelo, D., C. P. Pestana, and L. Gomez, 2016, Reverse time migration (rtm) using analytical wavefield and causal imaging condition: 78th Annual Intern. Conference and Exibition, EAGE, Extended Abstract, **Th P1 01**.

Shen, P. and U. Albertin, 2015, Up-down separation using hilbert transformed source for causal imaging condition: SEG, Technical Program Expanded Abstracts, 4175–4179.

Tessmer, E., 2011, Using the rapid expansion method for accurate time-stepping in modeling and reverse-time migration: Geophysics, **76**, S177–S185.

Yoon, K. and K. J. Marfurt, 2006, Reverse-time migration using the poynting vector: Exploration Geophysics, **37**, 102–107.

Zhang, Y. and J. Sun, 2009, Practical issues in reverse time migration: True amplitudes gathers, noise removal and harmonic-source encoding: First Break, 26, 19–25.

Zhang, Y. and G. Zhang, 2009, One-step extrapolation method for reverse time migration: Geophysics, **74**, A29–A33.